Timing analysis with *INTEGRAL*: comparing different reconstruction algorithms

V. Grinberg[1,2], I. Kreykenbohm[1], F. Fürst[1], J. Wilms[1], K. Pottschmidt[3,4], M. Cadolle Bel[5], J. Rodriguez[6], D.M. Marcu[3,4,7], S. Suchy[8], A. Markowitz[8], M.A. Nowak[9]

[1] *Remeis-Observatory/ECAP/FAU, Bamberg, Germany*
[2] *USM/LMU, Munich, Germany*
[3] *CRESST/NASA-GSFC, Greenbelt, MD, USA*
[4] *UMBC, Baltimore, MD, USA*
[5] *ESAC, Madrid, Spain*
[6] *DSM/DAPNIA/SAp, CEA Saclay, France*
[7] *GMU, Fairfax, VA, USA*
[8] *CASS/UCSD, La Jolla, CA, USA*
[9] *MIT/Chandra X-ray Center, Cambridge, MA, USA*

Abstract

INTEGRAL is one of the few instruments capable of detecting X-rays above 20 keV. It is therefore in principle well suited for studying X-ray variability in this regime. Because *INTEGRAL* uses coded mask instruments for imaging, the reconstruction of light curves of X-ray sources is highly non-trivial. We present results from the comparison of two commonly employed algorithms, which primarily measure flux from mask deconvolution (`ii_lc_extract`) and from calculating the pixel illuminated fraction (`ii_light`). Both methods agree well for timescales above about 10 s, the highest time resolution for which image reconstruction is possible. For higher time resolution, `ii_light` produces meaningful results, although the overall variance of the lightcurves is not preserved.

Keywords: timing analysis, instrumentation and methods, lightcurves, data extraction

1 Introduction

The *INTEGRAL* satellite is one of the few instruments designed for the detection of X-rays above 20keV with a good time resolution. It offers a unique opportunity for timing studies in this regime though the exact analysis at high time resolution remains a challenge. In coded mask instruments like the IBIS telescope aboard the *INTEGRAL* the source radiation is modulated by a mask. Each source will cast a shadow image (shadowgram) – the combined shadowgram is recorded in the detector plane. To obtain the original image the detected flux distribution has to be deconvolved in an analytically and computationally non-trivial process which is highly CPU-intensive.

For the resonstruction of lightcurves two algorithms are commonly employed: `ii_lc_extract` deconvolves shadowgrams for each time and energy bin, where the lightcurve is extracted. `ii_light` calculates the lightcurves primarily from the pixel illuminated fraction (PIF, number between 0 and 1 for given source expressing the degree of illumination of a detector pixel). Both are included in the *INTEGRAL* Off-line Scientific Analysis (OSA) software package.

In the following we compare the two extraction mechanisms and discuss their advantages and shortcomings (Sec. 2) and then assess the suitability of `ii_light` for high time resolution analysis (Sec. 3). A short summary of the results and the implications for further timing analysis with *INTEGRAL* are given in Sec. 4

2 Comparison between different lightcurve extraction algorithms

To reduce the influence of the selected field on the results of the lightcurve extraction, we perform the comparison on two different fields. Figure 1 shows a comparison of significance mosaics obtained during the Cyg X-1 and GRS 1915+105 *INTEGRAL* key programme in the 20–40 keV energy band with the source in the fully coded field of view (FOV), i.e. to a maximum pointing offset of 4.5°,

from 15 science windows (ScWs) from revolution 628 and 26 ScWs from revolution 852, respectively. Cyg X-1 (countrate ~ 100 cps) is significantly brighter than GRS 1915+105 (~ 40 cps). While both fields are comparable regarding the sources taken into account for our extractions (named boxes, $\sigma_{\text{detection}} \geq 6$, cps ~ 0.5–4.5), the field of GRS 1915+105 is crowded with ~ 35 weak sources (marked with $\times$, $1 \leq \sigma_{\text{detection}} < 6$), while the field of Cyg X-1 shows only ~ 20 of those.

Figure 2 shows the correlation between the results obtained with `ii_light` (OSA 7 version) and `ii_lc_extract` (OSA 8 version) for sources in the fully coded field of view in the 18–50 keV and 20–50 keV band for Cyg X-1 and GRS 1915+105 (revolutions and ScWs as for mosaic images), respectively. At a 10 s time resolution `ii_lc_extract` fails to detect the respective sources in several timebins, resulting in datapoints with zero countrate and error (red circles), which are excluded from our analysis. `ii_lc_extract` **does not allow for a much higher time resolution than 10 s.** `ii_light` systematically underestimates the countrate. The 10 s lightcurves (cyan circles) are however well **linearly correlated** with a bestfit slope of 1.05 ± 0.01 for Cyg X-1 and 1.15 ± 0.01 for GRS 1915+105. Fits to individual ScW-averaged countrates (black circles) in both cases show a different linear correlation with a lower slope and a significant offset. Given the good correlation for the non-averaged lightcurves and the fact, that the average datapoints lie well on the 10 s lightcurve fits, we are inclined to attribute this to the low number of ScWs analysed. More data covering a greater range in countrates will shed light on this issue.

[2] analysed the performance of `ii_light` on all available *INTEGRAL* Crab data and found that `ii_light` **underestimates the countrates by about 5%**, consistent with our results. We attribute the different ratios of `ii_light` and `ii_lc_extract` results for Cyg X-1 and GRS 1915+105 to the differences in the fields: in a more crowded field like the one of GRS 1915+105 a signal is more likely to be assigned to the wrong source.

3 High Time Resolution with ii_light

For the following section we use all ScWs from revolution 628 where Cyg X-1 is in the fully or partially coded FOV, i.e., science windows with a pointing offset of up to $\sim 15°$.

Histograms (width 1 cps) of the `ii_light` lightcurves for Cyg X-1 (Fig. 3) and Gaussian fits to them show that though the scatter increases with the time resolution, the routine produces meaningful results. The centers of the Gaussians fit components (dashed lines) are well consistent with each other. The FWHM of the Gaussians increases by a factor of ~ 3 for one order of magnitude increase in time resolution, consistent with the decreasing SNR. The deviations from the Gaussian shape are explained by the high intrinsic variability of the source of $> 25\%$ over the 3 days of the *INTEGRAL* revolution 628 as seen in Fig. 4. Note also that Fig. 4 supports the finding that `ii_light` underestimates the source flux - the different time resolutions are, however, consistent among each other and **reproduce the shape of the lightcurve well.**

Comparing the ratio between averaged countrates for individual ScWs of the `ii_light` lightcurves to the fluxes from the image extraction, we see no offset angle dependency as reported by [2]. The respective means of the ratios (dotted lines) agree well and indicate an offset of $\sim 5\%$, consistent with the linear correlation presented above for the fully coded FOV.

The power spectrum densities (PSDs) calculated from the above discussed `ii_light` lightcurves are shown on Fig. 6. For such PSDs calculated in Leahy normalizazion, the Poisson noise level should be equal to 2, independent of the countrate of the source. It can, however, clearly be seen here that even at as high frequencies as a few Hz, the PSD flattens out at a value of ~ 80 rms^2/Hz. This is consistent with the findings of [1] for Vela X-1, where the Poisson noise contributes as much as 100 rms^2/Hz at a given frequency.

Our PSDs for different time resolutions agree reasonably well with each other in shape (for exact timing studies longer periods than a single revolution would be necessary to reduce the uncertainities). Note that [3] also found consistent PSD shapes comparing ISGRI and RXTE-PCA 15–70 keV data for Cyg X-1. So while a better noise correction is required, `ii_light` **lightcurves are still well suited for timing studies with a 10 s to 0.1 s resolution in the regime above 20 keV.**

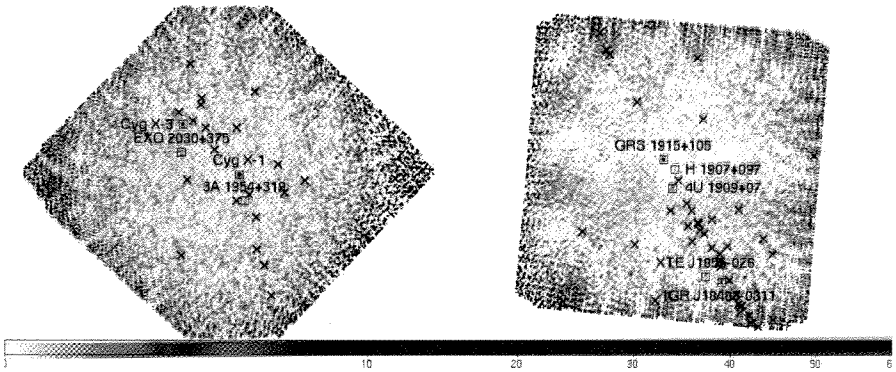

Figure 1: Intensity mosaics of the fields of Cyg X-1 and GRS 1915+105 in the 20–40 keV band.

4 Summary and Conclusions

We have shown that it is possible to perform timing studies with a resolution of up to 0.1 s with *INTEGRAL* when using the `ii_light` tool. Although `ii_light` (OSA 7 version) systematically underestimates the countrates when compared to more exact deconvolution algorithms (which do not allow better time resolution than 10 s even for bright sources such as Cyg X-1) the differences can in principle be assessed and taken into account. The correlation between the countrates is linear with the slope apparently depending on the field under consideration. A more detailed analysis of sources in different fields will allow to better quantify this linear correlation.

The countrates of the `ii_light` lightcurves follow a Gaussian distribution around the mean value. We do not see a dependency on the pointing offset angle of the observation.

PSDs calculated from these lightcurves with different time resolutions agree well with each other, the noise does however show anomalous behaviour which has also been observed by [1].

References

[1] Fürst F., Kreykenbohm I., Pottschmidt K., et al., 2010, A&A, 2010, A&A 519, 37

[2] Kreykenbohm I., Wilms J., Kretschmar P., et al., 2008, A&A 492, 511

[3] Pottschmidt K., Wilms J., Nowak M., et al., 2006, Advances in Space Research 38, p. 1350

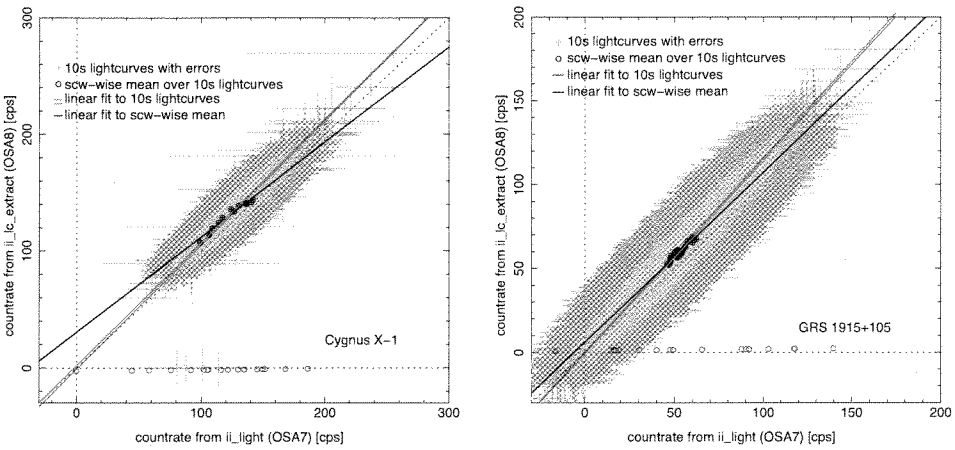

Figure 2: Scatterplots for countrates obtained with `ii_lc_extract` and `ii_light`

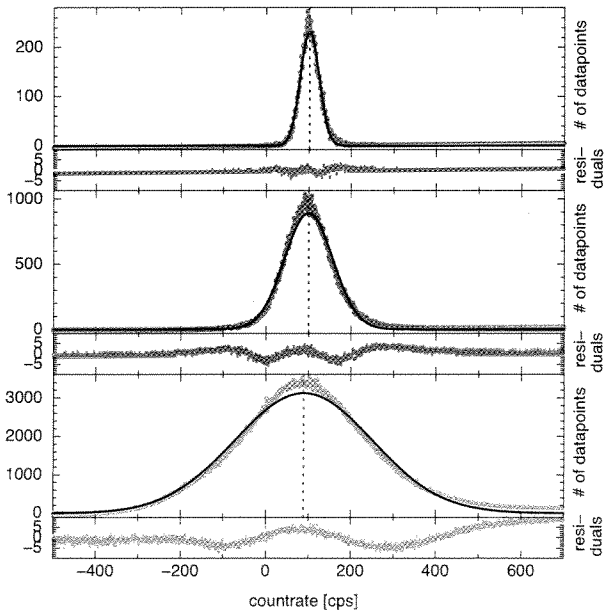

Figure 3: Histograms (width 1 cps) of the `ii_light` lightcurves of revolution 628 with 10 s (upper panel), 1 s (middle panel) and 0.1 s (lower panel) time resolution and up to $\sim 15°$ pointing offset angle in the 20–40 keV band of Cyg X-1 and Gaussian fits to them. The dotted lines indicate the centers of the Gaussians.

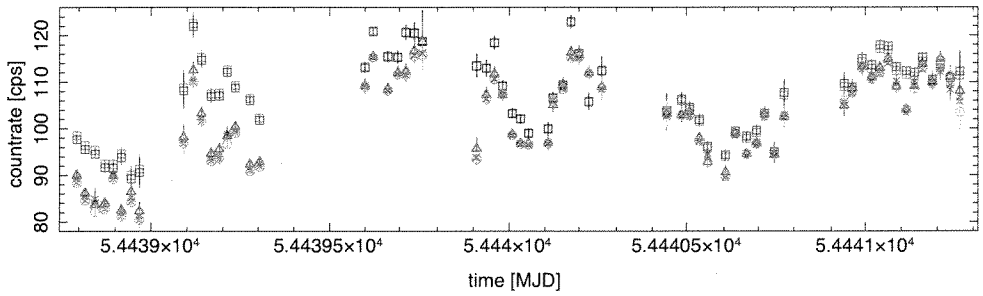

Figure 4: Fluxes from image extraction (box; deconvolution algorithm consistent with `ii_lc_extract`) as well as averaged countrates for individual ScW of the `ii_light` lightcurves with 10 s (triangle) 1 s (x) and 0.1 s (ciccle) time resolution in the 20-40 keV energy band

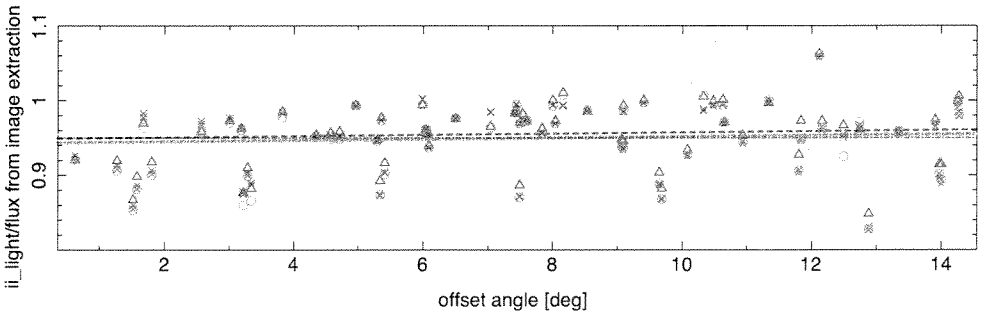

Figure 5: The ratio between averaged countrates for individual ScWs of the `ii_light` lightcurves with 10 s (triangle), (x) and 0.1 s (circle) time resolution in the 20-40 keV energy band to the fluxes from the image extraction in dependency of the pointing offset angle of the science window.

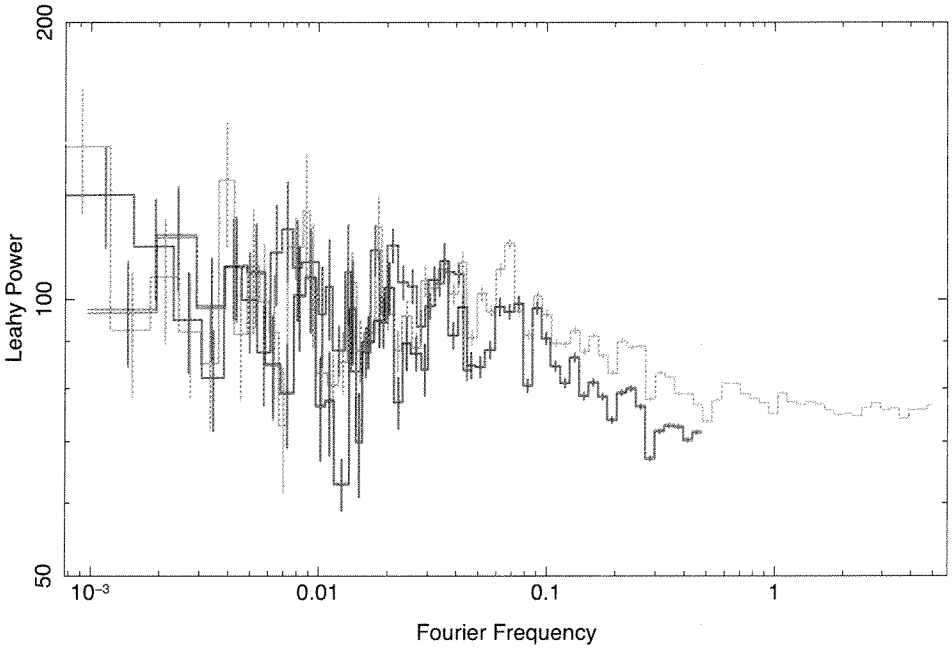

Figure 6: Power spectrum densities (PSDs) for Cyg X-1 presented here for the lightcurves with 10 s (red), 1 s (blue) and 0.1 s (brown) time resolution in the 20–40 keV energy band in the Leahy normalization.